Biophysics / Biophysique

Monitoring the interaction between DNA and a transcription factor (MEF2A) using fluorescence correlation spectroscopy

Guillaume Octobre, Claudie Lemercier, Saadi Khochbin, Michel Robert-Nicoud, Catherine Souchier [*]

Inserm U309, institut Albert-Bonniot, domaine de la Merci, 38706 La Tronche cedex, France

Abstract

Fluorescence correlation spectroscopy (FCS) is an analytical method that allows distinguishing different populations of fluorescent probes in solution and provides data on their concentrations and their diffusion coefficients. FCS was used to characterize the interaction of the transcription factor (MEF2A) with its DNA target sequence. The myocyte enhancer factor 2 (MEF2) belongs to the MADS-box family and activates transcription of numerous muscle genes during myogenesis. Measurements were made using TAMRA-labelled oligonucleotide duplexes derived from a wild type (WT) or a mutated MEF2 target gene. Binding of the protein to the WT DNA resulted in significant changes of the diffusion. Specificity of the interaction was confirmed using the mutated DNA. Bound to free probe ratios were determined at different MEF2A concentrations and the apparent equilibrium dissociation constant K_D for the full-length MEF2A was estimated. ***To cite this article: G. Octobre et al., C. R. Biologies 328 (2005).***
© 2005 Académie des sciences. Published by Elsevier SAS. All rights reserved.

Résumé

Suivi d'une interaction ADN–facteur de transcription (MEF2A) par spectroscopie à corrélation de fluorescence. La spectroscopie à corrélation de fluorescence (FCS) est une méthode qui permet de distinguer en solution plusieurs populations de molécules fluorescentes et d'estimer leurs concentrations et leurs constantes de diffusion. La FCS a été utilisée pour caractériser l'interaction entre un facteur de transcription (MEF2A) et sa séquence cible sur l'ADN. Le facteur de transcription MEF2 *Myocyte enhancer factor 2* appartient à la famille des protéines à MADS-box et active la transcription de plusieurs gènes musculaires pendant la myogenèse. Des mesures FCS ont été réalisées sur des oligonucléotides double brin marqués au TAMRA et correspondant à la séquence consensuelle (WT) ou mutée (Mut) du site de liaison ADN/MEF2A. La liaison MEF2A sur son site d'interaction (WT) se traduit par un allongement significatif du temps de diffusion. La spécificité de l'interaction a été confirmée par l'utilisation de la séquence mutée (Mut). La FCS a permis d'évaluer le rapport libre/lié pour plusieurs concentrations de MEF2A et la constante de dissociation apparente K_D. ***Pour citer cet article : G. Octobre et al., C. R. Biologies 328 (2005).***
© 2005 Académie des sciences. Published by Elsevier SAS. All rights reserved.

* Corresponding author.
  E-mail address: Catherine.Souchier@ujf-grenoble.fr (C. Souchier).

1. Introduction

Fluorescence correlation spectroscopy (FCS) is an analytical method that allows distinguishing different populations of fluorescent probes in solution and provides data on their concentrations and their diffusion coefficients [1–4]. The main advantages of FCS are: the capability to perform rapid measurements, the small amount of material required and no needs for radioactive labelling. Typically, analyses are performed at a concentration of 4 nM in a 20-μl volume during 30 s. FCS is based on the analysis of fluctuations in fluorescence intensity that results from diffusion of molecules in and out an open small confocal volume (<1 fl). Data are analysed by autocorrelation function and fitted to diffusion models. FCS thus renders possible quantitative study of molecular interactions and binding kinetics. The DNA–protein binding processes can be followed by monitoring the change in translational diffusion time of fluorescent double-stranded oligonucleotides upon specific binding to the proteins.

In the present study, FCS was used to characterize the MEF2A–DNA binding process. MEF2 ('Myocyte Enhancer Factor 2') was originally identified as a muscle-specific DNA-binding factor that recognizes a conserved A/T-rich DNA sequence in the muscle creatine kinase (MCK) enhancer [5]. MEF2 has also been shown to have significant roles in neurons and other cell types [6,7]. MEF2 belongs to the MADS-box transcription factor family [8–11]. The MADS domain comprises 57 amino acids located at the extreme N-terminus of MEF2. This motif serves as a minimal DNA-binding domain and the additional adjacent 29 amino acid extension, referred to as the MEF2 domain, plays an important role in DNA-binding high affinity [12]. In contrast to the MADS motif, the MEF2 domain is specific to MEF2 proteins, which are encoded by four different genes in mammals, *Mef2A*, *Mef2B*, *Mef2C* and *Mef2D*. MEF2 binds as a dimer to the core sequence (C/T)TA(A/T)4TA(A/G) found in numerous promoter of muscle specific genes [10,13]. Structural studies have shown that MEF2A makes contact both in the major and in the minor grooves of the DNA. DNA interaction is mediated exclusively by residues located in the MADS-box domain, whereas dimerization involved both the MADS-box and the MEF2 domains [14,15].

The goal of our study was to characterize the MEF2A–DNA equilibrium binding constant using FCS. A 23-mer DNA, containing a MEF2A consensus binding site, was labelled with TAMRA (6-carboxytetramethylrhodamine) fluorochrome and the binding process was monitored by FCS.

2. Materials and methods

2.1. Purification of MEF2A protein

Human MEF2A cDNA was amplified by PCR from pMT2-MEF2A plasmid [3] using the following oligonucleotides, 5′ to 3′: sense CATG<u>CCATGG</u>CCACCATG-GGGCGGAAGAAAATAC (NcoI site underlined) and antisense CCG<u>CTCGAG</u>GGGTCACCCACGCGTCCA-TC (XhoI site underlined). A Kozak sequence is present between the NcoI site and the initiation methionine codons in the sense primer. The PCR product was cut with NcoI and XhoI and ligated in pET28a vector (Novagen) in frame with the C-terminal 6-Histidine tag. His-MEF2A was produced in *E. coli* BL21 upon isopropyl-1-thio-ß-D-galactopyranoside (IPTG) induction. Bacteria were lysed in 50 mM Tris pH 8 solution containing 300 mM NaCl, 0.5% NP40 and 1 mM PMSF and sonicated. Soluble proteins were then incubated with NiTA agarose beads (Qiagen) in the presence of 15 mM imidazole. After extensive washes, bound proteins were eluted with 250 mM imidazole and dialyzed against 20 mM Tris pH 7.5 solution containing 10% glycerol and 1 mM DTT, at 4 °C. The purified proteins were analysed by SDS-PAGE and Coomassie blue staining or by Western blot using an anti-Histidine (PentaHis, Qiagen) or an anti-MEF2 antibody (C21, SantaCruz). Immunoreactive proteins were detected by chemiluminescence (ECL, Amersham Biosciences). For the estimation of MEF2 diffusion time, the protein was labelled using the 'fluorolink Cy5 monofunctional dye 5-pack' (Amersham-Pharmacia).

2.2. Oligodeoxyribonucleotides

The wild-type (WT) and the mutant (Mut) DNA used in the assays were derived from the mouse muscle creatine kinase (MCK) promoter: WT Oligo: 5′ TAMRA-CTCGCT**CTAAAAATAA**CCCTGTC 3′ and its complementary strand without label; Mut. Oligo:

5′ TAMRA-CTCGCT**CTAA**ggc**TAA**CCCTGTC 3′ and its complementary strand. Nucleotides in bold represent the MEF2 binding site [3], mutated nucleotides are in lower case. These HPLC-purified 23-mer DNAdeoxyribonucleotides were purchased from Sigma-Genosys. Annealing was performed by heating to 80 °C a solution of 1:1 ratio of the complementary strands, followed by slow cooling to room temperature. The efficiency of the annealing procedure was verified by electrophoresis of the oligonucleotide duplexes on acrylamide gel. The TAMRA-labelled DNAs were purified through a Sephadex G-50 column (Amersham) for removing the free fluorochrome.

2.3. FCS analysis

FCS study was performed on the Confocor 2 system (Carl Zeiss, Jena, Germany) using a 40 X water immersion C-Apochromat objective lens (N.A. = 1.2). The measurements were carried out at room temperature in eight-well Lab-Tek I chambered coverglass (Nalge Nunc International). The 543-nm He–Ne laser beam was focussed into 20-µl solutions at 180 µm over the cover glass. The fluorescence emission was collected through a pinhole and a 560-nm-long pass filter. Photon counts were detected by an Avalanche PhotoDiode (APD) at 20 MHz for 30 s. For each sample, FCS measurements were repeated 10 times. The data evaluation was performed using the Zeiss FCS Fit software. Most of the intensity autocorrelation curves were fitted using a free diffusion model with three components: the fluorochrome alone, the labelled DNA and the fluorescent DNA–protein complex. Preliminary studies enabled us to fix the diffusion time values of the first two components and the percentage of the first component (fluorochrome). Moreover, a calibration step with 4 nM Rhodamine 6G (R6G) made it possible to evaluate the size of the confocal volume (≈ 0.4 fl).

2.4. Interaction assays

Interaction assays were performed at room temperature in the following binding buffer (25 mM Hepes pH 7.9, 50 mM KCl, 0.5 mM EDTA pH 8, 5 mM MgCl$_2$, 5 mM DTT, 10% glycerol, 0.002% NP40). 5 to 400 nM of MEF2A proteins (typically: 100 nM) were mixed with 5 nM DNA and 0.5 µg poly (dI)(dC) in 20 µl of binding buffer.

2.5. Theoretical calculation

Diffusion constants were compared to theoretical values calculated assuming globular or rod-like macro-

molecules. The diffusion constants of the globular molecules were calculated using:

$$D = \frac{kT}{6\pi\eta n} \tag{1}$$

with T the absolute temperature, k the Boltzman constant, r the molecular hydrodynamic radius and η the viscosity of the medium. The radius r was calculated from the molecular mass m of the molecule: $r = \sqrt[3]{(3mN_A^{-1})/(4\pi\rho)}$, with N_A the Avogadro number and ρ the mean density of the molecule.

The theoretical diffusion coefficient D of the oligonucleotide was calculated using [16]:

$$D = \mu_{\text{chain}}T \tag{2}$$

where $\mu_{\text{chain}} = k(\ln(L/d) + \nu)/(3\pi\eta L)$ for a cylinder with L the length of the DNA, d its diameter. For the end-effect correction factor, ν, the theory proposed for the diffusion of rod-like macromolecule was used [17]:

$$\nu = 0.312 + 0.565/(L/d) - 0.1/(L/d)^2$$

taking into account the length (L, 78.2 Å for a 23 mer) and the diameter of the rod ($d = 23.8$ Å).

2.6. Determination of interaction parameters by FCS

Given that MEF2 proteins are assembled as homo- and heterodimers and that dimerisation is a prerequisite for DNA-binding [9,11], and given the short size of the oligonucleotide, we have considered the binding of one protein dimer to a single binding site. The DNA-binding reaction may be represented by:

$$\text{DNA}^* + \text{Dimer} \underset{k_{\text{diss}}}{\overset{k_{\text{ass}}}{\rightleftarrows}} \text{Complex}^* \tag{3}$$
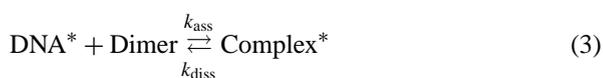
DNA* and Complex* are both fluorescent (*), and their concentrations may be evaluated using FCS. Therefore, the binding constant K can be evaluated according to the following equation:

$$K = \frac{[\text{Complex}^*]}{[\text{DNA}^*][\text{Dimer}]} = \frac{k_{\text{ass}}}{k_{\text{diss}}} = \frac{1}{K_D} \tag{4}$$

Moreover, the complex fraction, as expressed by Eq. (5), can be rearranged as Eq. (6). Therefore, this form was used for the estimation of the dissociation constant (K_D), from non-linear curve fitting (Y; f([free dimer]).

$$Y = \frac{[\text{Complex}^*]}{[\text{Complex}^*] + [\text{DNA}^*]} \tag{5}$$

$$Y = \frac{K \times [\text{Dimer}]}{1 + K \times [\text{Dimer}]} \tag{6}$$

Excel (Microsoft, USA) and Origin (OriginLab, USA) software were used for data evaluation.

3. Results and discussion

3.1. Purification of MEF2A from E. coli

MEF2A protein was produced from *E. coli* upon IPTG induction. Bacteria lysates were then purified on nickel affinity column by the mean of a 6-histidine tag. The His tag was positioned at the carboxy terminus of the protein in order to minimize the possible interference with the N-terminal DNA-binding and dimerization domains (Fig. 1A). Coomassie blue staining of purified MEF2A showed the presence of the expected 62-kDa full length protein (Fig. 1B). Two minor bands were co-purified with His-MEF2A, one migrating around 50 kDa and the other close to 80 kDa. Like full length MEF2A, the 50-kDa protein was recognized by an anti-histidine and an anti-MEF2 antibody directed against the C-terminus of the protein (Fig. 1C). Therefore, the 50-kDa protein is likely to represent a truncated MEF2 protein. The identity of the 80-kDa protein is unknown. The DNA-binding ability of the purified MEF2A was verified by electrophoretic mobility shift assays using the MEF2 binding site derived from the muscle creatine kinase promoter that was used in subsequent FCS analyses (see sequence in materials and methods). These assays indicated that His-MEF2A was capable of binding to the MEF2 binding site, whereas His-MEF2A binding was not observed with a mutated DNA probe (data not shown). Thus, purified His-MEF2A appeared to be functional for DNA-binding and the protein was used in FCS experiments to characterize the interaction between MEF2 and its cognate DNA sequence.

3.2. FCS Analysis

3.2.1. Diffusion parameters of free molecules

The diffusion coefficients of the different fluorescent molecules used in the assays were first estimated individually. Measurements were performed with about 4 nM sample solutions in PBS containing or not 10% glycerol. Autocorrelation curves are shown in Fig. 2 and the diffusion coefficients are listed in Table 1. As expected, mean diffusion times through the confocal volume increased both with molecular weight (Fig. 2, compare **2** to **3**) and medium viscosity (compare **1** to **2**) and were correlated with a decrease in diffusion coefficients (Table 1). The addition of glycerol led to a 1.2 fold increase of the diffusion times due to the change in viscosity. The medium viscosity was evaluated to 1.3 by
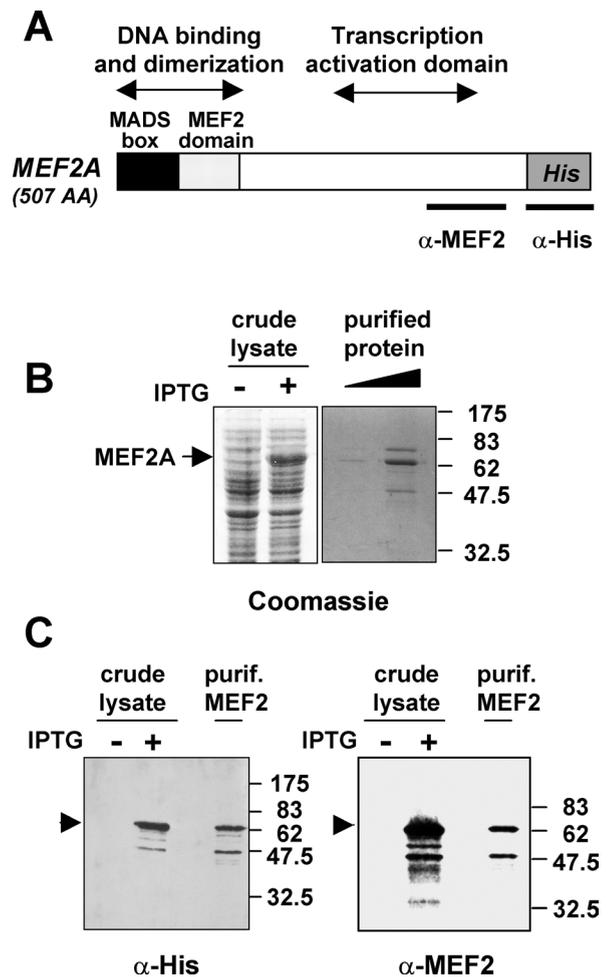

Fig. 1. (**A**) Functional map of the MEF2A protein. The MADS box and MEF2 domains (86 amino acids), necessary for efficient DNA-binding and dimerisation, are present at the N-terminus of MEF2, whereas the major transcription activation domain is located between amino acid 274 and 373. The epitopes recognized by the antibodies used in this study are indicated. (**B**) Production and purification of His-MEF2A in *Escherichia coli*. SDS-PAGE gels with Coomassie blue staining show the induction of MEF2A in crude extract of bacteria treated (+) or untreated (−) with IPTG, and the purified protein used in FCS experiments. (**C**) Western blot analysis of crude extracts from induced (+)/uninduced (−) bacteria and of the purified protein with anti-His (left) and anti-MEF2 antibodies (right).

comparing the diffusion measurements of TAMRA and Cy5 with theoretical data assuming a globular model (Eq. (1)). In our subsequent interaction assays, Rhodamine 6G, TAMRA and TAMRA–DNA were analysed at the beginning of each experiment. Rhodamine 6G analysis was used to estimate the confocal volume. On average, at 543 nm, the confocal volume was close to 0.4 fl with an axial axis of 0.23 μm, and a longitudinal axis of 2.7 μm. At the longest 633-nm wavelength used for Cy5 excitation, the axial axis was larger,

Table 1
Diffusion coefficients of the individual components

	Molecular mass (g/mol)	Diffusion time (μs)		Diffusion coefficient ($cm^2 \, s^{-1}$)	
		in PBS	in 10% glycerol	Measured in 10% glycerol	Theoretical (1.3 viscosity)
Rhodamine 6G	479	38.6 ± 2.6[*]	50.3 ± 2.7	$2.9 \pm 0.3 \times 10^{-6}$	2.9×10^{-6}
TAMRA	430	35.0 ± 2.6	50.1 ± 3.2	$2.8 \pm 0.3 \times 10^{-6}$	2.8×10^{-6}
Cy5	792	62.5 ± 1.9	80.1 ± 1.4	$2.8 \pm 0.2 \times 10^{-6}$	2.6×10^{-6}
Cy5-MEF2A	54 800 [°]	–	411 ± 63	$5.5 \pm 0.3 \times 10^{-7}$	6.3×10^{-7}[°]
					5.0×10^{-7}[°°]
TAMRA–DNA (23 mer)	14 614	188 ± 29	220 ± 23	$6.3 \pm 0.5 \times 10^{-7}$	7.0×10^{-7}[**]

[*] Mean ± s.d., [°] monomer, [°°] dimer, [**] without TAMRA, rod-like model.
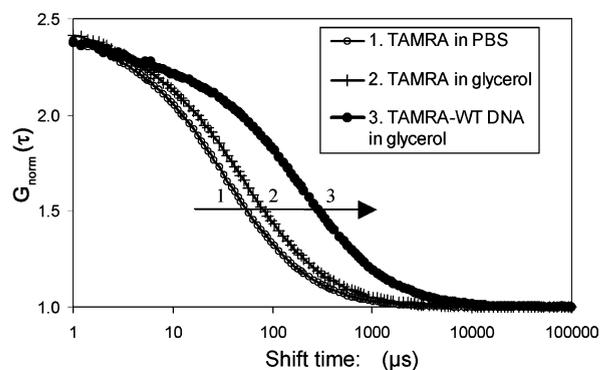

Fig. 2. Fluorescence correlation spectroscopy of free and TAMRA-labelled DNA. The WT DNA derived from the muscle creatine kinase promoter contains a MEF2 binding site. The normalised autocorrelation curves are shown for: (**1**) TAMRA in PBS, (**2**) TAMRA in 10% glycerol, (**3**) TAMRA–DNA. The inflexion points correspond to the mean diffusion times. The diffusion time increased with viscosity (1 to 2) and with molecular weight (2 to 3).

about 0.3 μm. Corrections for the differences in volume were used to standardize the results. This explains why Cy5-MEF2A ($\lambda_{exc} = 633$ nm) and TAMRA–DNA ($\lambda_{exc} = 453$ nm) have different diffusion times but equal diffusion coefficients (Table 1). Moreover, slightly different diffusion coefficients of Cy5-MEF2A and the DNA reflect the differences both in molecular weight and in shape: globular vs. rod-like (Eqs. (1) and (2)). In summary, our results illustrate that, as expected, diffusion coefficients strongly depend on viscosity, molecular mass and overall shape of the molecules. In our assays, preliminary analysis of TAMRA and TAMRA–DNA allowed us to set their diffusion times at fixed values for the analysis of interaction. A stepwise procedure improved the quality of the fits with additional components. The analysis of labelled MEF2A was performed in order to get an estimation of the protein diffusion (= 411 μs); however, in the interaction experiment, the label was on the DNA and not on MEF2A protein.

The measured value is between the expected values for MEF2A dimer (451 μs) or monomer (357 μs), according to a globular model and under our experimental conditions at 633-nm excitation. However, due to the shape approximation involved in simple hydrodynamic models, FCS does not make it possible to discriminate, in our opinion, between monomer and dimer protein, only on the diffusion data. Our labelling process does not allow us to include additional data, such as concentration or count per molecule.

3.2.2. Interaction analysis between MEF2A and TAMRA-labelled DNA

Interaction assays were first performed using MEF2A at a concentration of 100 nM and the wild type DNA (WT DNA) or the modified sequence (Mut. DNA). The normalised autocorrelation curves obtained with the WT DNA differ significantly from those obtained with the Mut. DNA or the DNA alone (Fig. 3A). The differences between the curves were more pronounced using higher concentrations of MEF2A (Fig. 3B). In this assay, the curves were shifted to the right, indicating the presence of, at least, an additional slowly diffusing component. The Mut. and WT autocorrelation curves were similarly fitted using a two- or three-component free diffusion model. The diffusion times of the first two components (TAMRA alone and TAMRA–DNA) were fixed from the experiments using these components alone, performed at the beginning of each experiment (see Table 1, for example). A third component was only found in the WT DNA case. The diffusion time of this component was significantly higher than that of the free DNA (> 400 μs) and corresponds to the DNA–MEF2A complex. In the case of the Mut. DNA, the fit was not improved using the three component model, or the third diffusion value was close to that of the free DNA or the associated percentage was not significant. In summary, a significant diffusion change resulting from the binding
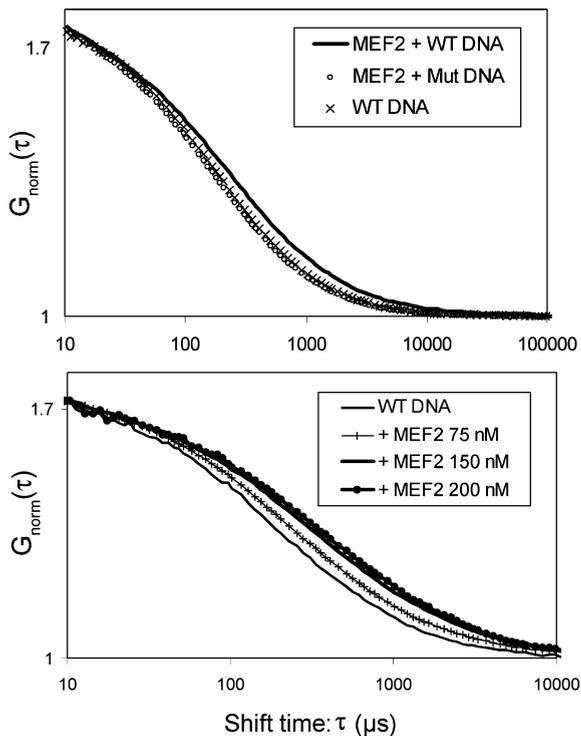
Fig. 3. Interaction between MEF2A and a TAMRA-labelled target DNA monitored by FCS. Experiments were performed with a fixed concentration of DNA (5 nM). (**A**) The normalised autocorrelation curve was shifted to the right by mixing MEF2A (100 nM) with the WT–DNA, reflecting the presence of a slower component. By contrast, no shift was observed with the DNA having MEF2-binding mutation site, its autocorrelation curve being essentially similar to that of the WT DNA alone. (**B**) With increasing amount of added MEF2A protein (0, 75, 150 and 200 nM), the proportion of the slowest component increased and the autocorrelation curves were shifted to the right.

of MEF2A to DNA was only observed with a consensus MEF2 binding site, whereas a mutated DNA sequence did not allow the interaction with MEF2A.

3.3. Binding constants

Interaction assays of MEF2A and DNA were performed using various MEF2A concentrations (5 to 400 nM). The results were adjusted using a three-component model: the fluorochrome, the fluorescent DNA and the MEF2A–fluorescent DNA complex. The complex ratios were estimated in each experiment and expressed relatively to the total concentration of MEF2A–TAMRA–DNA and TAMRA–DNA, excluding the free TAMRA fluorochrome (Eq. (5) in § *Material and methods*). The titration curve ($Y = f$[free protein]) was then non-linearly adjusted using the Levenberg–Marquardt algorithm (Origin software) (Fig. 4) and the apparent equilibrium binding constant
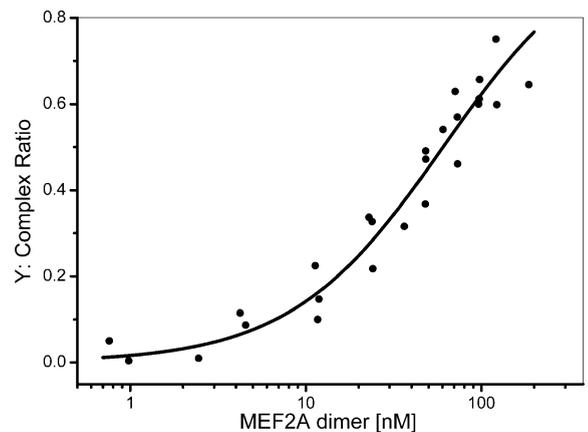

Fig. 4. Titration curve of MEF2A dimers for WT DNA (5 nM). MEF2A dimer concentration ranged from 0 to 200 nM. The protein-bound DNA fractions (Y) are plotted as a function of the protein dimer concentration in the binding medium. Each point represents the average of 10 measurements of 30 s. The solid line represents the fitted curve determined according to Eq. (3) in § *Material and methods* and using the Levenberg–Marquardt algorithm (Origin software).

(K_D) of MEF2A dimers was estimated to 60 ± 4 nM (Eq. (6), $\chi^2 = 0.003$). The best fit was found using the simple model (Eq. (6)), and cooperative binding was not observed, in agreement with crystallography data [14, 15]. A binding constant equal to 110 nM was reported for MEF2C [18,19], but a significantly higher affinity ($K_D = 0.5$ nM) was published for MEF2A [20]. This difference might be explained by the fact that, in this study, only the N-terminal region (amino acids 2–86) containing essentially the MADS-box and the MEF2 domain and another DNA length (60 mers) were used. Moreover, in our study, poly $(dI)(dC)$ was added in the interaction buffer to prevent non-specific binding. Precise estimation of theoretical diffusion values for DNA/protein complex is difficult; however the diffusion time of the complex (> 400 µs, typically 550 µs) is significantly higher than that of the free DNA and corresponds to the DNA–MEF2A complex with MEF2A most likely in the dimeric form. However, the presence of few DNA–multimer complex, corresponding to the second band showed by electrophoretic mobility shift assay by Berger et al. [20], or the contribution of the minor protein bands (Fig. 1) cannot be totally rejected. To gain further information, cross correlation [21–23] studies could be performed. Their main advantage would be to provide concentration and diffusion data both on the protein, the oligonucleotide and their interaction. However, exact standardization and the use of fluorochromes with shorter excitation wavelengths, such as FAM, for diminishing spectral crosstalk with Cy5, would be needed.

4. Conclusion

In conclusion, our study confirmed that FCS makes it possible to perform binding assays and to estimate the equilibrium binding constant (K_D) [24–29]. The main advantages of this technique are: few materials are required, no radioactive labelling is needed and the experiments are performed in solution. However, measurements are possible using one fluorescent component, only if there is a significant difference in mass between free and bound components. Moreover, FCS made it possible to acquire time series (every 1–2 s) and thus should render possible the estimation of kinetic data (k_{ass}, k_{diss}) when the interaction and the dissociation process are slow enough. However, modifications of the input system, such as automatic injection and mixing, would be necessary for monitoring the earliest time points.

In the case of MEF2A–DNA interaction, our results and those obtained for MEF2C [18,19] would suggest that MEF2 homodimers might bind to their DNA targets with a lower affinity than other MADS-box factor [30–32]. Differences in the ability to bend DNA were also observed within the MADS-box family. In contrast to Agamous, SRF and MCM1, which induce a 70° bend in the target DNAs [30,31,33], MEF2 proteins distort the DNA to smaller extent (15 to 19°) [9,14,15]. Moreover, crystallographic and NMR studies of MEF2A bound to DNA reveal that the MEF2 domain adopts a conformation considerably different from the corresponding region in SRF and MCM1 [15]. Altogether, affinity determination, kinetic parameters and structural analysis show that the MEF2 proteins represent a group of transcription factors with specific DNA-binding activities within the MADS box family.

Acknowledgement

References

[1] E.L. Elson, Fluorescence correlation spectroscopy measures molecular transport in cells, Traffic 2 (2001) 789–796.

[2] S.T. Hess, S. Huang, A.A. Heikal, W.W. Webb, Biological and chemical applications of fluorescence correlation spectroscopy: a review, Biochemistry 41 (2002) 697–705.

[3] E. Haustein, P. Schwille, Ultrasensitive investigations of biological systems by fluorescence correlation spectroscopy, Methods 29 (2003) 153–166.

[4] M. Gosch, R. Rigler, Fluorescence correlation spectroscopy of molecular motions and kinetics, Adv. Drug. Deliv. Rev. 57 (2005) 169–190.

[5] L.A. Gossett, D.J. Kelvin, E.A. Sternberg, E.N. Olson, A new myocyte-specific enhancer-binding factor that recognizes a conserved element associated with multiple muscle-specific genes, Mol. Cell. Biol. 9 (1989) 5022–5033.

[6] A. Han, J. He, Y. Wu, J.O. Liu, L. Chen, Mechanism of recruitment of class II histone deacetylases by myocyte enhancer factor-2, J. Mol. Biol. 345 (2005) 91–102.

[7] T.A. McKinsey, C.L. Zhang, E.N. Olson, MEF2: a calcium-dependent regulator of cell division, differentiation and death, Trends Biochem. Sci. 27 (2002) 40–47.

[8] F. Messenguy, E. Dubois, Role of MADS box proteins and their cofactors in combinatorial control of gene expression and cell development, Gene 316 (2003) 1–21.

[9] A.G. West, P. Shore, A.D. Sharrocks, DNA binding by MADS-box transcription factors: a molecular mechanism for differential DNA binding, Mol. Cell. Biol. 17 (1997) 2876–2887.

[10] Y.T. Yu, R.E. Breitbart, L.B. Smoot, Y. Lee, V. Mahdavi, B. Nadal-Ginard, Human myocyte-specific enhancer factor 2 comprises a group of tissue-restricted MADS box transcription factors, Genes Dev. 6 (1992) 1783–1798.

[11] P. Shore, A.D. Sharrocks, The MADS-box family of transcription factors, Eur. J. Biochem. 229 (1995) 1–13.

[12] J.D. Molkentin, B.L. Black, J.F. Martin, E.N. Olson, Mutational analysis of the DNA binding, dimerization, and transcriptional activation domains of MEF2C, Mol. Cell. Biol. 16 (1996) 2627–2636.

[13] V. Andres, M. Cervera, V. Mahdavi, Determination of the consensus binding site for MEF2 expressed in muscle and brain reveals tissue-specific sequence constraints, J. Biol. Chem. 270 (1995) 23246–23249.

[14] K. Huang, J.M. Louis, L. Donaldson, F.L. Lim, A.D. Sharrocks, G.M. Clore, Solution structure of the MEF2A–DNA complex: structural basis for the modulation of DNA binding and specificity by MADS-box transcription factors, EMBO J. 19 (2000) 2615–2628.

[15] E. Santelli, T.J. Richmond, Crystal structure of MEF2A core bound to DNA at 1.5-Å resolution, J. Mol. Biol. 297 (2000) 437–449.

[16] P.-G. de Gennes, Scaling Concepts in Polymer Physics, Cornell University Press, 1979.

[17] M. Tirado, C. Martinez, J. Garcia de la Torre, Comparison of theories for the translational and rotational diffusion coefficients of rod-like macromolecules. Application to short DNA fragments, J. Chem. Phys. 81 (1984) 2047–2052.

[18] D. Meierhans, R.K. Allemann, The N-terminal methionine is a major determinant of the DNA binding specificity of MEF-2C, J. Biol. Chem. 273 (1998) 26052–26060.

[19] D. Meierhans, M. Sieber, R.K. Allemann, High affinity binding of MEF-2C correlates with DNA binding, Nucleic Acids Res. 25 (1997) 4537–4544.

[20] I. Berger, C. Bieniossek, C. Schaffitzel, M. Hassler, E. Santelli, T.J. Richmond, Direct interaction of Ca^{2+}/calmodulin inhibits histone deacetylase 5 repressor core binding to myocyte enhancer factor 2, J. Biol. Chem. 278 (2003) 17625–17635.

[21] N. Baudendistel, G. Muller, W. Waldeck, P. Angel, J. Langowski, Two-hybrid fluorescence cross-correlation spectroscopy detects

protein–protein interactions in vivo, Chem. Phys. Chem. 6 (2005) 984–990.

[22] S.A. Kim, K.G. Heinze, K. Bacia, M.N. Waxham, P. Schwille, Two-photon cross-correlation analysis of intracellular reactions with variable stoichiometry, Biophys. J. 88 (2005) 4319–4336.

[23] K. Rippe, Simultaneous binding of two DNA duplexes to the NtrC-enhancer complex studied by two-color fluorescence cross-correlation spectroscopy, Biochemistry 39 (2000) 2131–2139.

[24] H. Xu, J. Frank, U. Trier, S. Hammer, W. Schroder, J. Behlke, M. Schafer-Korting, J.F. Holzwarth, W. Saenger, Interaction of fluorescence labeled single-stranded DNA with hexameric DNA–helicase RepA: a photon and fluorescence correlation spectroscopy study, Biochemistry 40 (2001) 7211–7218.

[25] F.W. Sevenich, J. Langowski, V. Weiss, K. Rippe, DNA binding and oligomerization of NtrC studied by fluorescence anisotropy and fluorescence correlation spectroscopy, Nucleic Acids Res. 26 (1998) 1373–1381.

[26] J. Vercammen, G. Maerstens, M. Gerard, E. De Clercq, Z. Debyser, Y. Engelbroghs, DNA-induced polymerization of HIV-1 integrase analyzed with fluorescence correlation spectroscopy, J. Biol. Chem. 277 (2002) 3845–3852.

[27] T. Kobayashi, N. Okamoto, T. Sawasaki, Y. Endo, Detection of protein–DNA interactions in crude cellular extracts by fluorescence correlation spectroscopy, Anal. Biochem. 332 (2004) 58–66.

[28] J. Wolcke, M. Reimann, M. Klumpp, T. Gohler, E. Kim, W. Deppert, Analysis of p53 'latency' and 'activation' by fluorescence correlation spectroscopy. Evidence for different modes of high affinity DNA binding, J. Biol. Chem. 278 (2003) 32587–32595.

[29] T. Yakovleva, A. Pramanik, T. Kawasaki, K. Tan-No, I. Gileva, H. Lindegren, U. Langel, T.J. Ekstrom, R. Rigler, L. Terenius, G. Bakalkin, p53 Latency. C-terminal domain prevents binding of p53 core to target but not to nonspecific DNA sequences, J. Biol. Chem. 276 (2001) 15650–15658.

[30] J.L. Riechmann, M. Wang, E.M. Meyerowitz, DNA-binding properties of *Arabidopsis* MADS domain homeotic proteins APETALA1, APETALA3, PISTILLATA and AGAMOUS, Nucleic Acids Res. 24 (1996) 3134–3141.

[31] L. Pellegrini, S. Tan, T. Richmond, Structure of serum response factor core bound to DNA, Nature 376 (1995) 490–497.

[32] T.B. Acton, H. Zhong, A.K. Vershon, DNA-binding specificity of Mcm1: operator mutations that alter DNA-binding and transcriptional activities by a MADS box protein, Mol. Cell. Biol. 17 (1997) 1881–1889.

[33] S. Tan, T.J. Richmond, Crystal structure of the yeast MATa2/MCM1/DNA ternary complex, Nature 391 (1998) 660–666.